



# Effect of atmospheric pollutants on the corrosion of high power electrical conductors: Part 1. Aluminium and AA6201 alloy

Rosa Vera <sup>a</sup>, Diana Delgado <sup>a</sup>, Blanca M. Rosales <sup>b,\*</sup>

<sup>a</sup> *Corrosion Laboratory, Institute of Chemistry, Pontificia Universidad Católica de Valparaíso, Chile*

<sup>b</sup> *CIDEPINT, Av. 52 s/n, entre 121 y 122, B1900AYB La Plata, Argentina*

Received 31 August 2004; accepted 1 November 2005

Available online 2 February 2006

---

## Abstract

The aim of this study was to evaluate the joint effect of marine and industrial pollutants on the atmospheric corrosion of aluminium and its AA6201 alloy. Weight loss was determined after 4, 11, 16 and 24 months exposure being morphology and attack intensity analysed through SEM–EDX. Both materials showed the most intense attack for the highest SO<sub>2</sub> contents. Good correlation among weight loss, attack depth and tensile strength to rupture with time and with pollutant contents was determined for both materials in most sites. The cause for low aggressiveness of the heaviest Cl<sup>-</sup> polluted atmosphere on aluminium was electrochemically demonstrated.

© 2006 Elsevier Ltd. All rights reserved.

*Keywords:* A. Aluminium; A. AA6201 alloy; B. SEM; B. EDX; C. Atmospheric corrosion

---

## 1. Introduction

Aluminium and its alloys are today the most used metals in high power electrical transmission lines and nets of distribution. Their resistance to corrosion results from highly adherent hydrated alumina films (Al<sub>2</sub>O<sub>3</sub>·3H<sub>2</sub>O) formed under atmospheric exposure. These strongly passivating continuous films, non-soluble in water, act as a barrier against

---

\* Corresponding author. Tel./fax: +54 11 4782 9921.

E-mail addresses: [rvera@ucv.cl](mailto:rvera@ucv.cl) (R. Vera), [brosales@fibertel.com.ar](mailto:brosales@fibertel.com.ar) (B.M. Rosales).

corrosive agents [1–3]. The presence of pollutants ( $\text{Cl}^-$  and  $\text{SO}_2$ ), however, significantly affect the corrosion kinetics forming less compact, more soluble corrosion products. Consequently materials undergo localised attack with significant loss of mechanical resistance [4–6]. This leads to premature failure even in materials with good mechanical properties, as the AA6201 (Al–Si–Mg) alloy.

Given that atmospheric corrosion does not occur by immersion but in the presence of small amounts of water from the atmosphere as rain or dew condensed on the metallic surfaces, localised attack is generally found on areas with the longest times of wetness (TOW). Atmospheric pollutants also settle on surfaces producing different salt concentrations which allow corrosion reactions. The heterogeneous distribution of those substances contributes to a localised character of atmospheric corrosion with consequent attack morphology. Their relative intensity depends on the type and concentration of the dissolved pollutant in the thin water layers available on metallic surfaces.

The properties of the corrosion products formed depend on the chemical composition and metallurgical history of the metal [7–9] as well as on the atmospheric conditions determined by meteorological variables, as wet and dry cycles and pollutant concentrations [10]. However, the available pollutants alone do not determine atmospheric aggressiveness but also a concentrate electrolyte should remain during an appreciable fraction of time to produce the joint effect. The protectiveness of the corrosion products formed depends on their chemical composition, conductivity, adherence, compactness, solubility, hygroscopic character and morphology [7,11–13].

Hence the importance of focusing in the effect of diverse combinations of the atmospheric factors affecting the corrosion rate of metallic wires widely used for electricity transmission.

## 2. Experimental

Exposure of the materials studied during this work took place in atmospheric test stations at 17 marine and marine-industrial sites. Selection of the test sites involved distances to the sea from 60 m to 4000 m and different altitudes from 0 m to 180 m over sea level (osl). Besides, stations were installed at distances ranging between 500 m and 1500 m from an industrial plant, the only  $\text{SO}_2$  pollutant source.

Tests samples were 99.0% aluminium and the AA6201 alloy (97.62% Al, 0.7% Si and 0.9% Mg). The initial metals condition was as received, stranded wires of 2.25 mm and 3.00 mm diameter, respectively, cut to 1000 mm length. The specimens were formed as open helices rolling the wires around a 24 mm diameter mandrill. Contact with other material or with adjacent spires that could form crevice was avoided. Fixed by their isolated ends at  $45^\circ$  angle to the horizon, two replicates of each material were exposed at the outdoor atmospheres, during 4, 11, 16 and 24 month periods.

Ambient pollutant concentrations and meteorological parameters as well as the respective corrosivity classification of the atmospheres are summarised in Table 1. The outdoor exposition as well as the methodology for the atmospheric characterisation and weight loss determinations followed ISO 9223 to 9226 [14–17] and ISO 8407 [18] standards, respectively.

Morphology in plan and cross-section of attack was analysed through scanning electron microscopy using a SEM Philips 515, coupled to an EDAX 9100 analyser for elemental characterisation. Polished cross-section samples of both materials were also studied by optical microscopy at the 17 test sites after different exposure periods.

Table 1  
Location and ambient characteristics of the 17 test sites

Type of atmosphere	Station (no.)	Exposure site	Sea dist. (m)	Height osl (m)	[Cl <sup>-</sup> ] (mg m <sup>-2</sup> day <sup>-1</sup> )	ISO Cat. <sup>a</sup>	[SO <sub>2</sub> ] (mg m <sup>-2</sup> day <sup>-1</sup> )	ISO Cat. <sup>a</sup>
Marine	18	Concón	2190	25	17.2	S <sub>1</sub>	19.1	P <sub>1</sub>
Marine	6	Concón	4060	25	17.4	S <sub>1</sub>	29.8	P <sub>1</sub>
Marine	20	Reñaca	930	125	19.0	S <sub>1</sub>	21.1	P <sub>1</sub>
Marine	23	Reñaca	1810	145	21.1	S <sub>1</sub>	33.3	P <sub>1</sub>
Marine	29	Reñaca	200	125	27.3	S <sub>1</sub>	19.2	P <sub>1</sub>
Marine	28	Reñaca	0	0	44.5	S <sub>1</sub>	9.4	P <sub>0</sub>
Marine	24	San Antonio	1051	69	20.1	S <sub>1</sub>	1.2	P <sub>0</sub>
Marine	12	San Antonio	227	62	21.4	S <sub>1</sub>	4.1	P <sub>0</sub>
Marine	15	San Antonio	14 770	180	22.1	S <sub>1</sub>	3.6	P <sub>0</sub>
Marine	27	San Antonio	269	21	31.0	S <sub>1</sub>	5.1	P <sub>0</sub>
Marine	2	San Antonio	4	0	131.8	S <sub>2</sub>	7.2	P <sub>0</sub>
Marine-indust.	10	Ventana	760	30	32.0	S <sub>1</sub>	86.8	P <sub>3</sub>
Marine-indust.	14	Ventana	1220	41	28.3	S <sub>1</sub>	94.4	P <sub>3</sub>
Marine-indust.	4	Ventana	1980	47	18.6	S <sub>1</sub>	103.8	P <sub>3</sub>
Marine-indust.	13	Ventana	600	13	17.5	S <sub>1</sub>	240.4	>P <sub>3</sub>
Marine-indust.	9	Ventana	660	12	21.3	S <sub>1</sub>	282.3	>P <sub>3</sub>
Marine-indust.	5	Ventana	690	11	20.4	S <sub>1</sub>	651.2	>P <sub>3</sub>

<sup>a</sup> According to ISO 9224 standard [15].

X-ray analysis was applied to the corrosion products formed on the exposed samples after different periods in both types of atmospheres. The equipment used was a SIEMENS D 5000 with Cu K $\alpha$  radiation and a graphite monochromator 40 kV/30 mA, in the scanning range 05–70°.

Follow up of both materials residual mechanical resistance after the exposure periods in several atmospheres was performed on weathered wire samples with a Losenhausen machine model 10 Tm through tensile strength to rupture.

Anodic and cathodic polarisations were applied on triplicate weathered aluminium samples from sites 2 and 27, and on non-exposed witness samples. The anodic curves were obtained in 0.1 M NaNO<sub>3</sub> passivating electrolyte after solutions deaeration by 99.99% N<sub>2</sub> bubbling and the cathodic curves in air saturated solutions, at 20 °C, and 100 mV min<sup>-1</sup> potential scan rate. A conventional Pyrex glass cell with Pt counter electrode and a saturated calomel electrode as reference, through a Luggin capillary, were used.

### 3. Results

Location and ambient characteristics of the test sites are summarised in Table 1. Temperature (*T*), relative humidity (RH), predominant winds and rains of the area involving the 17 test sites are included in Fig. 1(a)–(c). The traverse board shown in Fig. 2 evidences that SW yearly predominant winds supply salt fog from the sea depending on the shore line distance and more or less free access. Fig. 3 shows a croquis of the Fifth Region sea-shore zone of Valparaíso, Chile (Lat. 32°S, Long. 71°W) where the test sites were mounted.

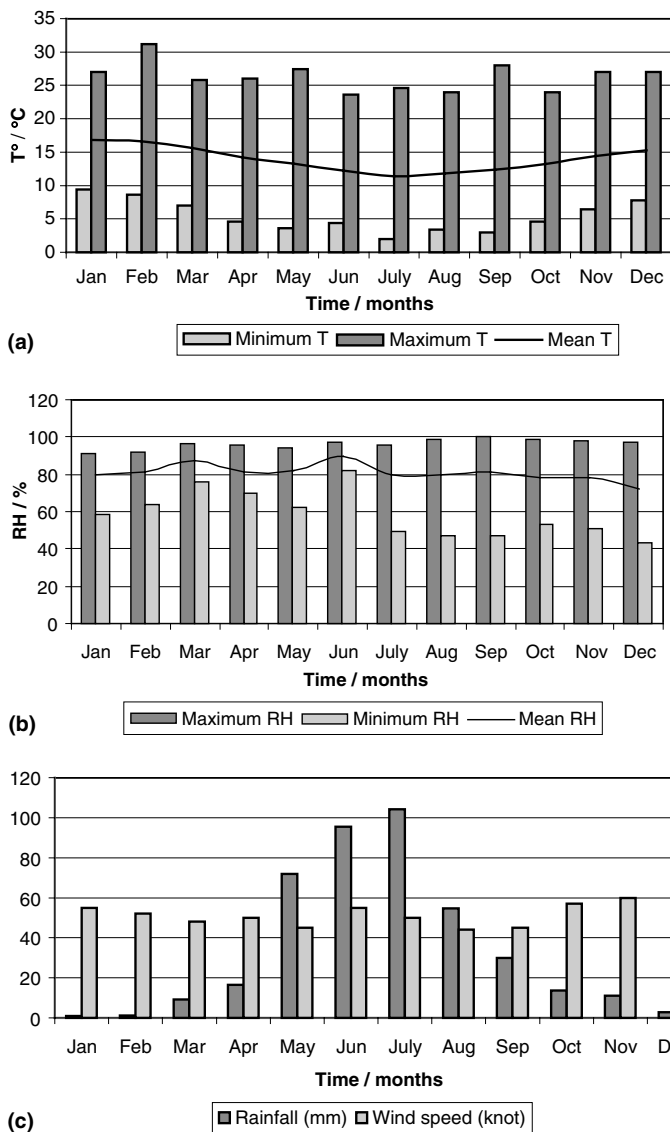


Fig. 1. Meteorological parameters in the Fifth Region, Chile, with time (period 1970–2003). (a) Extreme and mean temperature. (b) Extreme and mean relative humidity. (c) Mean rainfall and maximum wind speed.

The main components of the corrosion products determined through X-ray diffraction are shown in Table 2 for each material and type of atmosphere.

Figs. 4 and 5 show the mass loss in function of time for both aluminium and the AA6201 alloy at the test sites in marine and marine-industrial environments, respectively.

In Fig. 6 the panoramic aspect of samples exposed to the heaviest polluted marine-industrial atmosphere 5 reveals changes in both materials at 4 and 11 month exposure times, including EDX of the corrosion products on pure aluminium samples.

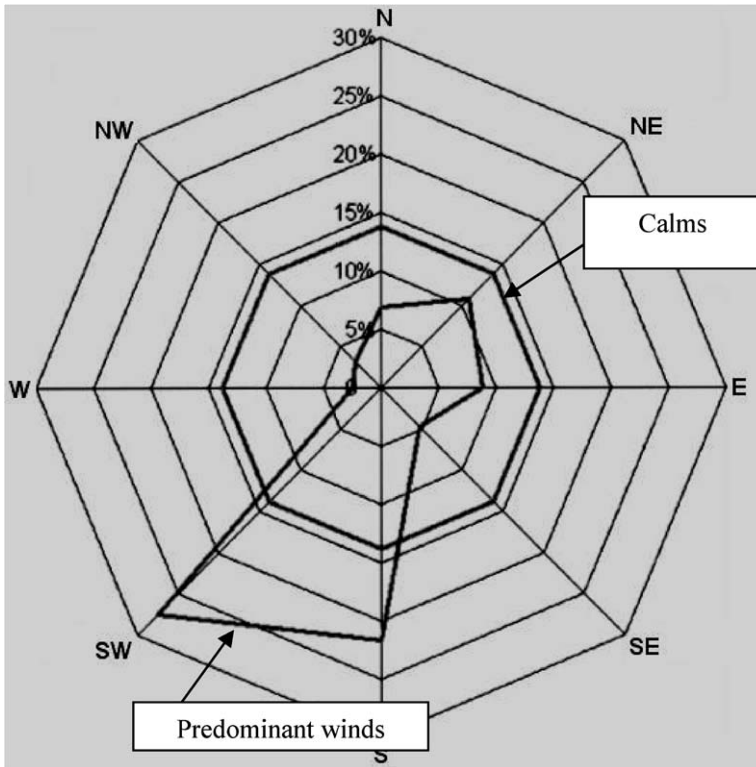


Fig. 2. Traverse board of Valparaiso, Chile.

Table 3 shows EDX of alloy samples after 4 and 11 month exposure in the marine sites 2 and 27. In Fig. 7, polished transverse cross-section of both materials can be observed after exposure in the same marine atmospheres of very distinct aggressiveness. Anodic and cathodic polarisation of weathered aluminium evidenced different behaviour after 24 month exposure at the marine test sites 2 and 27, as compared to non-exposed samples, in Fig. 9.

#### 4. Discussion

According to Koppen's classification [19] this region has moderate temperatures due to the oceanic influence with a long dry Summer and rainy Winter season, designed Cs. Table 1 shows that three test sites close to the SO<sub>2</sub> pollution source surpass the maximum SO<sub>2</sub> atmospheric concentration defined by ISO 9225 standard as P3 category. Accordingly, very high corrosion rates were expected at those sites.

The complex infrastructure mounted did not only result in different proportions of marine and industrial pollutant combinations but it also provided different amounts of salt fog to each test site atmosphere. In fact, the diversity in distances to the sea shore and height over sea level of the 17 sites allowed also evaluation of the variable pollutants effect once dissolved during diverse TOWs by water condensation on metallic surfaces.

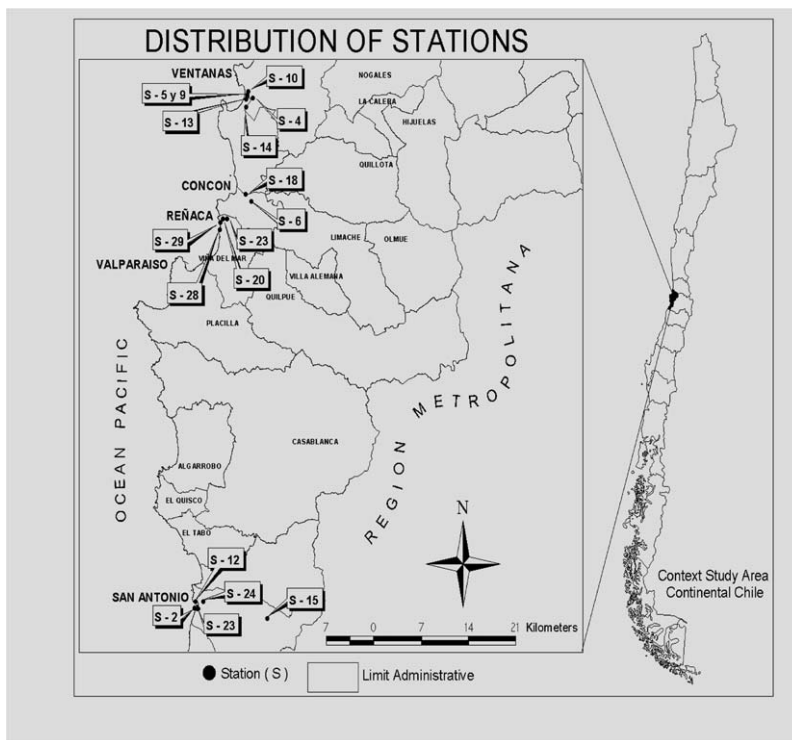


Fig. 3. Croquis of the test stations geographic locations.

Table 2

X-ray diffraction of the corrosion products formed on aluminium and on the AA6201 alloy in the marine and marine-industrial test sites after different exposure times

Aluminium		AA6260 alloy	
Marine sites	Marine-indust. sites	Marine sites	Marine-indust. sites
Quartz (SiO <sub>2</sub> )	Albite (NaAlSi <sub>3</sub> O <sub>8</sub> )	Quartz (SiO <sub>2</sub> )	Albite (NaAlSi <sub>3</sub> O <sub>8</sub> )
Sodium chloride (NaCl)	Aluminium oxichloride (AlOCl)	Sodium chloride (NaCl)	Aluminium oxichloride (AlOCl)
Albite (NaAlSi <sub>3</sub> O <sub>8</sub> )	Quartz (SiO <sub>2</sub> )	Albite (NaAlSi <sub>3</sub> O <sub>8</sub> )	Quartz (SiO <sub>2</sub> )
Aluminium oxide (Al <sub>2</sub> O <sub>3</sub> )		Iron chloride (FeCl <sub>2</sub> )	
Iron–silicon hydrated oxide (Fe <sub>2</sub> O <sub>3,90</sub> SiO <sub>2</sub> H <sub>2</sub> O)			
Aluminium–hydrogen silicate (H–Al <sub>2</sub> O <sub>3</sub> –SiO <sub>2</sub> )			

#### 4.1. Weight-loss analyses

Good correlation between mass loss and exposure time was always found, while the relationship was not so direct with respect to the atmospheric Cl<sup>-</sup> and SO<sub>2</sub> deposition rates. In fact, for similar low chloride contents the measured corrosion rates were almost always controlled by the SO<sub>2</sub> concentration, as shown in Fig. 4(a) for sites 18, 6, 20, 24, 23

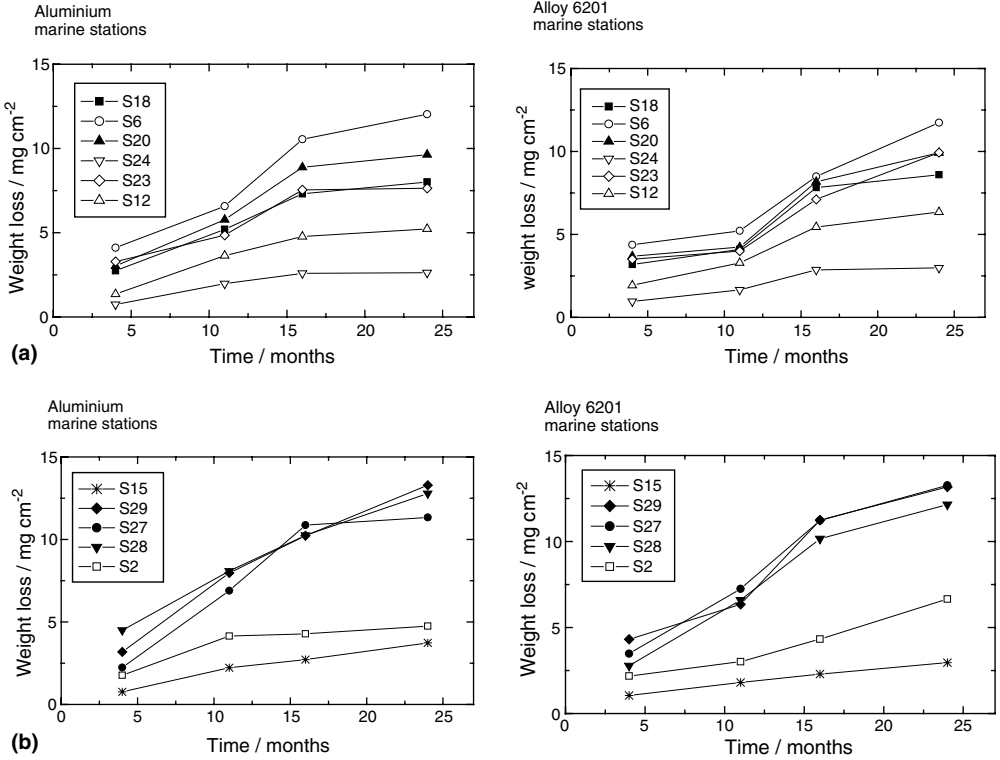


Fig. 4. Mass loss of aluminium and AA6201 alloy in function of exposure time in marine environments. (a) Sites 18, 6, 20, 24, 23 and 12, for lowest Cl<sup>-</sup> contents and various SO<sub>2</sub> contents. (b) Sites 15, 29, 28, 27 and 2, with higher Cl<sup>-</sup> than SO<sub>2</sub> contents.

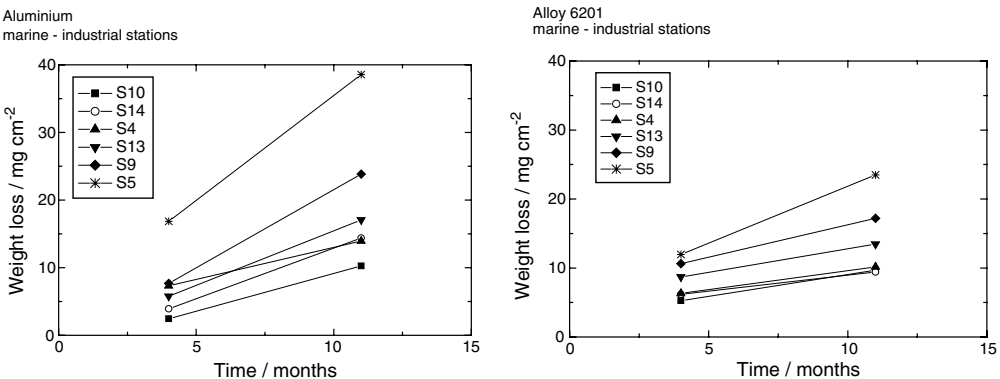
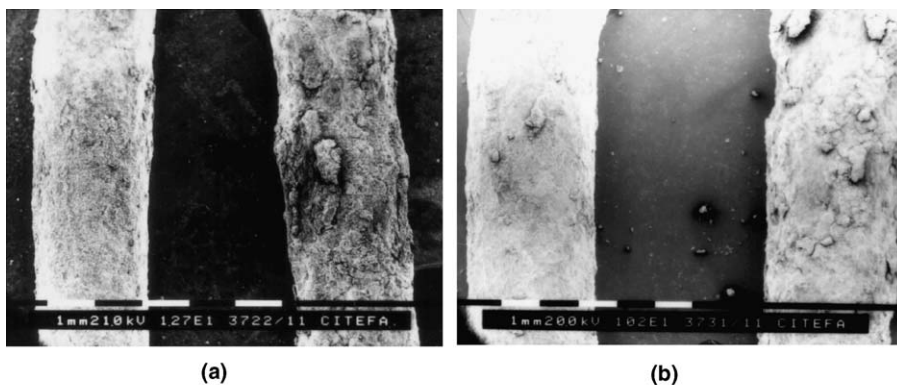


Fig. 5. Mass loss of aluminium and AA6201 alloy in function of the exposure time in marine-industrial stations, sites 10, 14, 4, 13, 9 and 5, with much higher SO<sub>2</sub> than Cl<sup>-</sup> content.

and 12, listed according to their increasing Cl<sup>-</sup> contents. But correlation disappeared when higher Cl<sup>-</sup> than SO<sub>2</sub> contents were involved, as shown in Fig. 4(b) for sites 15, 29, 28, 27



ELEM	WT %	WT %
	4 months	11 months
Na	7.02	2.21
Mg	2.27	1.72
Al	49.95	47.46
Si	5.59	9.39
S	19.37	16.50
Cl	0.52	0.65
K	1.49	0.56
Ca	2.21	1.68
Fe	2.37	7.19
Cu	4.89	10.35
Zn	4.32	2.94

(c)

Fig. 6. SEM aspect of aluminium and AA6201 samples after 4 and 11 months exposure in the marine-industrial environment of site 5 and EDX on pure Al corrosion products. (a) Pure aluminium. (b) AA6201 alloy. (c) EDX on (a).

and 2, also following increasing  $\text{Cl}^-$  levels. In sites with low  $\text{SO}_2$  content the atmospheric aggressiveness was proportional to the  $\text{Cl}^-$  concentration.

In the marine-industrial stations 10, 14, 4, 13, 9 and 5, with medium chloride levels and  $\text{SO}_2$  from high to very high contents, mass loss for aluminium and the alloy showed good

Table 3  
EDX on AA6201 alloy samples after 4 and 11 months exposure in sites 2 and 27

ELEM	Site (4 months) (WT%)		Site (11 months) (WT%)	
	2	27	2	27
Na	4.20	3.07	2.09	2.45
Mg	6.53	4.75	4.17	2.45
Al	18.63	13.67	25.55	41.30
Si	36.85	45.38	44.19	29.94
S	2.01	1.07	2.88	7.84
Cl	1.65	1.55	0.65	0.56
K	3.16	3.67	3.38	2.41
Ca	16.97	14.62	5.61	3.82
Fe	10.02	12.34	11.48	9.20

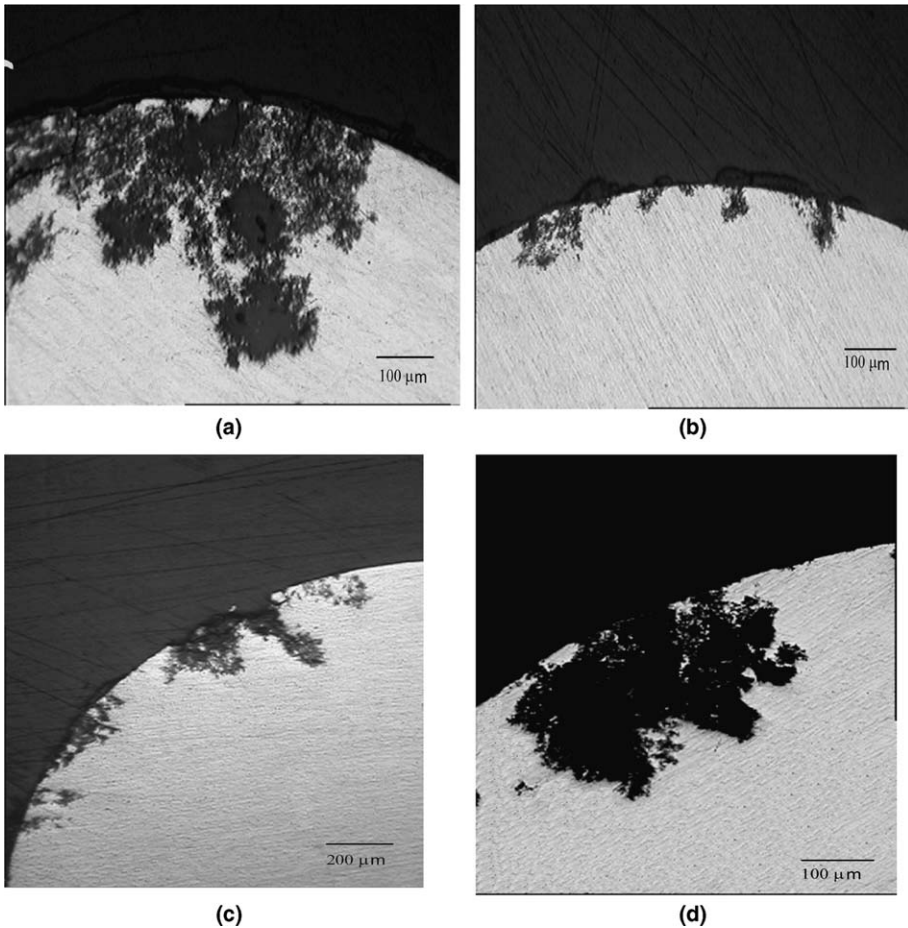


Fig. 7. Comparative SEM aspect in cross-section of aluminium and the AA6201 alloy after 4 and 11 month exposure periods in marine environments of sites 2 and 27. (a) Pure Al, site 2, 4 months. (b) Pure Al, site 27, 4 months. (c) Alloy, site 2, 4 months. (d) Alloy, site 2, 11 months.

correlation with SO<sub>2</sub> atmospheric concentration, as can be seen in Fig. 5. For such SO<sub>2</sub> levels minor changes in Cl<sup>-</sup> concentrations did not show any effect on the atmospheric aggressiveness.

Contrary to observed in marine test sites in these highly SO<sub>2</sub> polluted stations after 4 month exposure the alloy was more susceptible than aluminium, except towards the heaviest SO<sub>2</sub> polluted condition. In this environment the alloy presented 75% and 60% weight loss of shown by aluminium after 4 and 11 month exposure respectively. Presence of Si and Mg, the most commonly used alloying elements in aluminium industrial applications [3], could increase the initial alloy resistance only in the most extreme condition. The weight loss after 4 month exposure showed lower corrosion rate for pure aluminium than for the alloy, except in the most aggressive site 5. This relationship reverted since the second exposure period, the alloy showing lower corrosion rates than aluminium (Fig. 5).

#### 4.2. Morphology and chemical analyses

SEM aspect of both samples exposed to the heaviest marine-industrial polluted environment of site 5 (Fig. 6), confirm the weight loss results, showing larger amount of corrosion products on aluminium than on the alloy only after a 11 month exposure period.

Atmospheric corrosion of aluminium is generally localised, with initial isolate pitting on the metallic surface, leaving intact areas of metal in-between. Panoramic aspect of both materials attacked wires and polished transverse cross-sections can be observed after 4 and 11 month exposure in the most aggressive sites 5 and 2 both types of atmospheres (Figs. 6 and 7). The initial pits got further morphology with exposure time showing grain boundaries attack propagation with metals exfoliation, as was also found by other authors [20,21]. At this stage, the mass loss was not only caused by metal dissolution but it could also be due to non-corroded grain detachment (Figs. 6 and 7).

Pitting morphology was observed in cross-section of metal samples after the first exposure period and in the less polluted atmospheres, as shown in Fig. 7(b). For further exposure times and in heavier polluted environments the attack propagating through grain boundaries produced aluminium and alloy exfoliation, as in Fig. 7(a), (c) and (d). According to the relative amounts of both pollutant contents in the atmosphere different morphologies and attack depth were observed. In transverse cross-section heterogeneous distribution of attack penetration along the circumference was probably associated to the orientation of samples respect to both pollutant sources and uneven TOW as depicted in Fig. 7 for site 2 after 4 and 11 months exposure. Inversely, analogous analysis over both materials at station 27 showed more uniform and soft attack distribution all around the circumference (Fig. 7(b)). Random spatial distribution respect to corrosive agents was observed for its low SO<sub>2</sub> atmospheric content, in spite of its high chloride level. That could suggest that high Cl<sup>-</sup> contents would preferentially promote the attack nucleation while SO<sub>2</sub> would favour or synergise in depth propagation on both materials.

EDX on cross-section of samples after different exposure periods showed that the simultaneous presence of high sulphur and chloride compounds originated intense exfoliation and increase in the attack depth. This finding was more frequent for aluminium than for the alloy suggesting higher susceptibility for the pure metal than for the alloy.

Results shown in Table 2 from X-ray diffraction were similar for both materials after exposure in stations with the same type of pollutant, also identified and characterised by other authors [22–24] on the three layered structure formed by aluminium and its native

oxide, the corrosion layer and a surface contamination layer [25]. These results also revealed the presence of aluminium silicate.

#### 4.3. Solid pollutants

EDX on different samples (Fig. 6(c)) and (Table 3) evidenced high proportions of spurious elements. Amongst others, Na, Mg, Si, Fe and Ca are usually found in the corrosion products coming from the soil during outdoor tests.

That shows, as from X-ray results, that soil pollution must also be considered, because its inert components may act as crack and void filler in the corrosion product layers, increasing protectiveness (Fig. 8).

Some authors [5,26] observed on the contrary, that when a bare metal is exposed to dust polluted atmospheres capillary condensation on soil deposits would reduce the critical relative humidity for corrosion nucleation, enhancing the initial attack in the presence of  $\text{Cl}^-$  and/or  $\text{SO}_2$  contaminants.

#### 4.4. Anomalous weight losses

In the highest  $\text{Cl}^-$  polluted test station 2, both the aluminium and alloy samples presented very low weight losses. According to Fig. 4 they are in the same order of magnitude as in site 12 for all exposure periods, although the chloride content in station 2 is around sixfold that found in site 12. This unexpected behaviour was first attributed to fouling by atmospheric dust in samples collected at station 2, which could have increased protectiveness of the corrosion product layers their compacting by with inert solids.

However, after four month exposure the damage found in Fig. 7(a) was correlative with high  $\text{Cl}^-$  concentration, as compared with site 27 in Fig. 7(b). Not only the SEM aspect of the aluminium cross-sections shown, but also EDX on sites 2 and 27, in Table 3, suggested the need to replace that hypothesis by other also triggering higher corrosion products protectiveness on aluminium in site 2 than in 27.

The higher adherence of corrosion products on the aluminium samples from site 2 than from all other marine sites would have reduced the apparent weight loss in site 2.

According to previous results [27–29] corrosion products formed in some marine environments evidenced high protectiveness due to exceptionally enhanced adherence, which also showed high protectiveness increase with time.

This finding was verified during this study by a larger number of acid pickling immersions needed for corrosion products removal from aluminium samples of site 2 during weight loss determinations [18]. More intense acid treatment was always needed to dissolve the corrosion products formed on aluminium than on the AA6201 alloy and those formed on both of them when compared to other sites.

The weight loss graphs as a function of time shown in Fig. 4 allowed a careful analysis of each slope to evaluate the effects of pollutant concentrations. This is a valuable discussion tool because these slopes are inversely proportional to the protectiveness of the corrosion products formed on aluminium and on its alloy in both types of atmospheres, and allow comparison with those exposed in other sites for each period.

The yearly corrosion rate, which is the slope of the curves in Figs. 4 and 5, provide the most evident measure of the products protectiveness on both materials as a function of time, also occurring for Al, Zn [27], Cu [28] and steel [29], as previously demonstrated.

It also evidences the limiting pollutant content in the atmosphere, above which corrosion would continue on aluminium and/or its AA6201 alloy wires up to complete destruction. The electricity transmission lines would obviously be interrupted quite before in service condition, as soon as the first wire section becomes fractured under the tensile strength caused by its own weight.

#### 4.5. Protectiveness of corrosion products

The corrosion products formed always lead to corrosion rate decrease with respect to the initial bare metal surface (Figs. 8 and 9). Such decrease depends on the barrier effect that the product films cause. The nature and structure of the corrosion product components determine the layer efficiency to decrease the corrosive atmospheric agent access to the metal.

Determination of the slope of weight loss vs. time, as informed in previous papers [27–29], allows analysis of corrosion products protectiveness, especially reflecting its variation with time. They also provide experimental evidence of the unexpected inverse proportionality between metal weight loss and marine atmospheres corrosivity [27–29], as was demonstrated in Fig. 8 through an electrochemical technique.

The corrosion products protectiveness in less aggressive marine atmospheres increased with exposure time while in site 2, for the highest  $\text{Cl}^-$  content, they evidenced its highest protectiveness or adherence since the first exposure period.

Sample	$E_c$ (mV)	$I_c$ ( $\text{Acm}^{-2}$ )
Non exposed Al	-1068	$7.3 \times 10^{-4}$
Al S27	-860	$7.9 \times 10^{-6}$
Al S2	-728	$1.3 \times 10^{-6}$

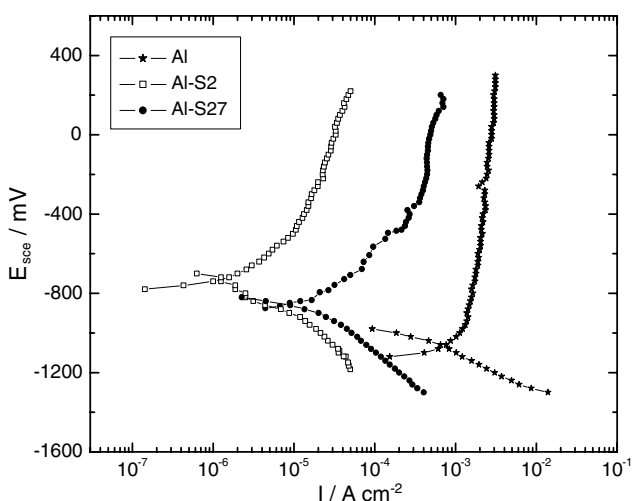


Fig. 8. Polarisation of aluminium, anodic in the absence of oxygen and cathodic in air saturated 0.1 M  $\text{NaNO}_3$  solution, after 24 months exposure in marine atmospheres of sites 2 and 27, as compared to non-exposed Al.

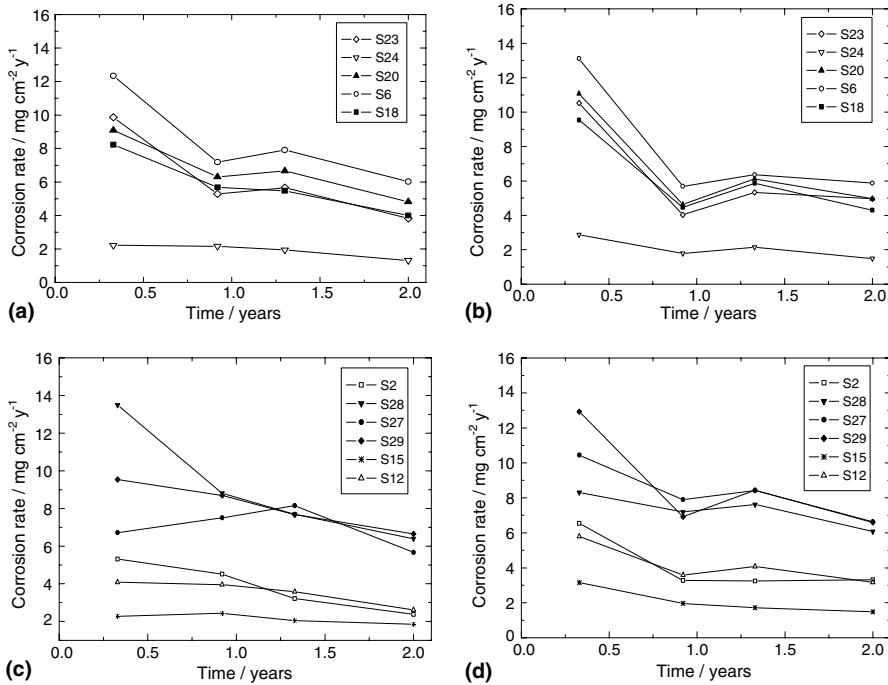


Fig. 9. Slope of graphs in Figs. 4 and 5 as a function of exposure time for both materials in the different types of atmospheres. (a) Al in marine sites 23, 24, 20, 6 and 18, with lowest Cl<sup>-</sup> and various SO<sub>2</sub> contents. (b) AA6201 alloy in marine sites 23, 24, 20, 6 and 18, with lowest Cl<sup>-</sup> and various SO<sub>2</sub> contents. (c) Al in marine stations 2, 28, 27, 29, 15 and 12, with higher Cl<sup>-</sup> than SO<sub>2</sub> contents. (d) AA6201 alloy in marine stations 2, 28, 27, 29, 15 and 12, with higher Cl<sup>-</sup> than SO<sub>2</sub> contents.

#### 4.6. Electrochemical analysis

Aluminium was electrochemically investigated after 24 month exposure to the marine polluted sites 2 and 27. Comparison of the corrosion products protectiveness thus determined allowed to explain the lower corrosion rate found in site 2 than in 27. Polarisation of aluminium in the anodic and cathodic directions in the 0.1 M NaNO<sub>3</sub> passivating electrolyte demonstrated higher protectiveness of the films formed at site 2, through lower current densities in spite of its highest atmospheric Cl<sup>-</sup> content (Fig. 8). Witness non-exposed aluminium samples evidenced the highest anodic and cathodic current densities due to their less protective original Al<sub>2</sub>O<sub>3</sub> film as compared to products formed in both test sites. Samples exposed at site 27 showed intermediate corrosion potential and current densities due to lower corrosion product protectiveness than those formed at site 2.

#### 4.7. Mechanical resistance

Fig. 10 shows the strength to rupture of both materials for different exposure times in various marine and marine-industrial atmospheres. It is clearly the inverse relation observed with the mass loss results. The mechanical resistance loss determined is a more sensitive and reliable parameter than the mass loss to foresee life expectancy of the alumin-

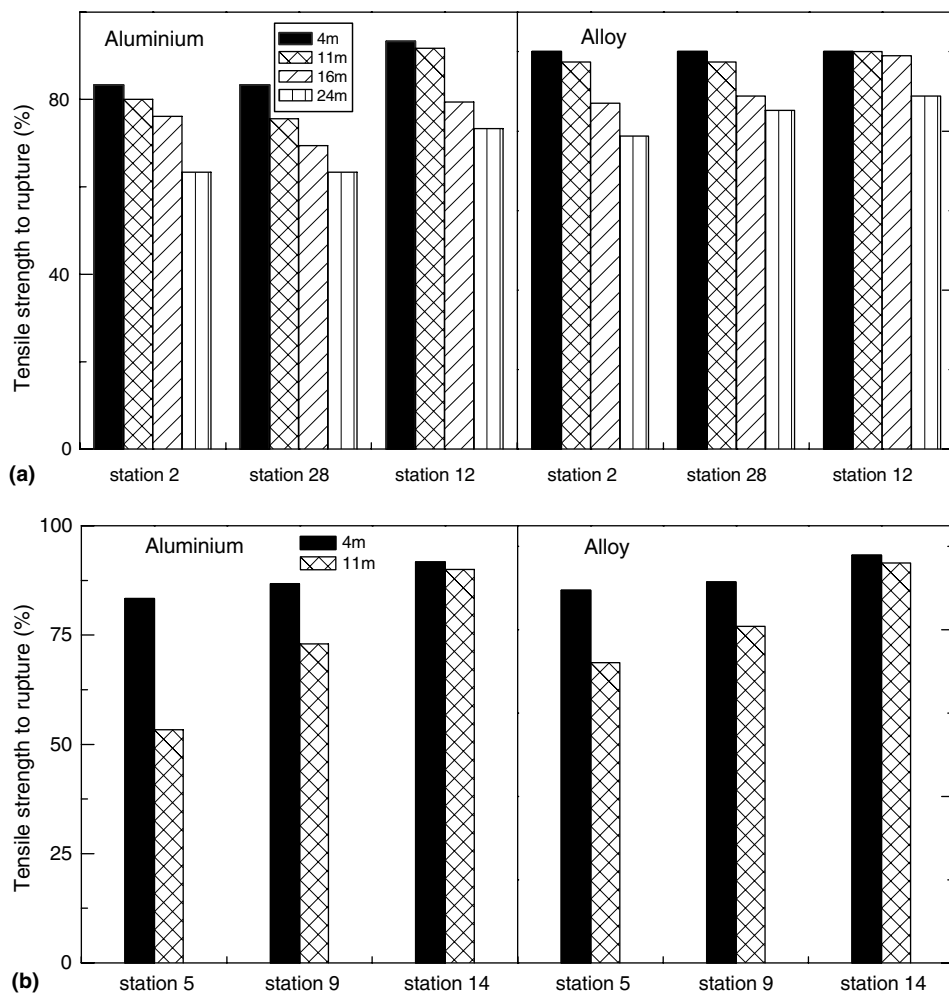


Fig. 10. Tensile strength to rupture of aluminium and AA6201 alloy after the different exposure periods in marine and marine-industrial environments. (a) Marine sites 2, 28 and 12. (b) Marine-industrial sites 5, 9 and 14.

ium base wires for electrical transmission. The strength due to the wire weight would enhance in service attack propagation on both metals by fresh intergranular areas exposure to corrosive agents.

The typical SEM aspect of fractographs is shown in Fig. 11. Close to the base of the shallow-broad surface, pits connect through intergranular attack showing evidence of ductile fracture. The ultimate tensile strength of the wires was increasingly reduced with exposure time through their effective section reduction caused by pitting and exfoliation.

In both types of environment the load resistance loss with exposure time was proportional to the  $\text{SO}_2$  atmospheric content. Corrosion assessment through this mechanical parameter also showed better behaviour for the alloy than for pure aluminium.

Curiously, the similar weight losses experienced for both metals at sites 2 and 12 were also reflected in similar strength to rupture in both sites. That seems to mean that the great



Fig. 11. Typical SEM fractographs of aluminium samples submitted to tensile strength.

corrosion products adherence or protectiveness leading to the low weight losses of both metals at site 2 would also determine improved mechanical resistance at that site.

#### 4.8. Evaluation of TOW effect

The TOW is a very sensitive parameter to sample shape, inclination and orientation [29]. Opposite to the frequently used flat samples, the exposed wires conformed as open helixes isolated from contact with any other material did not evidence such an almost homogeneous difference between sky and ground-ward flat surface. A helix, on the contrary presented all possible orientations and inclinations undergoing the effects of uneven pollutant deposition, washing-out by rains, sun drying, evaporation by winds and almost uniform dew condensation. Thus, there will be areas submitted to quite different measurable TOWs for the same meteorological data used in their estimate [15]. This was demonstrated in a previous paper in the same type of mixed polluted atmosphere for flat plain C steel samples, in which the exposition angle was the only variable, being the TOW produced the cause for noticeable differences in the corrosion rates [29]. However, higher relative pollutant accumulation between inner and outer phases of the corrosion film was found through EDX only on the inner more adherent layer than in the outer sky-ward face. This would be the main result allowing to discuss whether a synergistic or a competitive effect might be expected in mixed polluted atmospheres.

A detailed study comparing estimated to measured mean TOWs in five outdoor Argentine test stations allowed demonstrating that ISO standard estimations were affected by up to yearly 400% error [30].

But the TOW is not an exclusive result of environmental data triggering liquid water condensation on a surface. The metal on which water deposition occurs is determinant of its TOW, because of the colour, roughness and hygroscopic character of its surface product. Once corrosion initiated the surface properties of the compound formed enhance differences in the capacity of liquid water retention. Further reactions (precipitation, hydrolysis, etc.) increase heterogeneities contributing to even more scattered TOWs, locally enhancing differences in attack corrosion rate along the outer wire surface.

In the present study the low mean TOW of the whole region and atmospheric exposure time [29], estimated in around 20%, in compliance with ISO 9224 [15] standard results in too high pollutant content saturating solutions in one or both pollutants. This water

limitation does not completely allow manifesting the whole atmospheric contaminants content. The good correlation obtained for weight loss vs. the total pollutant levels in each test site not only for each period but also over the whole exposure time allows, to propose a cooperative effect of pollutants on both metals.

Previous results of steel corrosion rate also revealed this restriction in the contaminants effect associated to low mean TOWs, due to the low humidity content characteristic of the same Chilean region [29].

#### 4.9. Analyses of the effect of $Cl^-$ and $SO_2$ pollutant contents and other atmospheric parameters

To analyse the corrosive effect of joint pollutants the weight loss of aluminium and the alloy was represented as a function of their total concentration for the marine test sites after each exposure period in Fig. 12. The most relevant effects to discuss are:

1. The already analysed low weight loss of pure aluminium in atmosphere 2. Other marine sites showed reasonable increasing corrosion rates as a function of the total atmospheric pollutant concentration for all tested periods.
2. The sharp decreases at sites 15, 6, 18 and 23 after the 4 test periods for increasing total pollutants content. For a given salts concentration, the corrosive effect would be proportional to the time during which the available liquid water (TOW) allows enough salt dissolution to maintain corrosion reactions. Accordingly, increasing distances to the seashore line could cause decreasing TOWs that would strongly diminish metals weight loss at those sites. In consequence, most abrupt weight loss decreases must be expected, and they in fact occur, for stations located at greater distances from the sea than their 2 adjacent, as 24, 15, 18, 20, 6 and 23, in decreasing order.
3. On the contrary, a factor increasing the marine fog effect on a given site is its height over sea level, which allows a long distance effect due to less natural condensation barriers such as trees or buildings, causing salt and TOWs increases due to SW predominant winds from the ocean. This would increase losses in weight for sites 15, 23, 29, 20. However, deviation in weight loss duplicate determinations, exemplified in Fig. 13, limits any discussion intending further exploitation of the measured data.

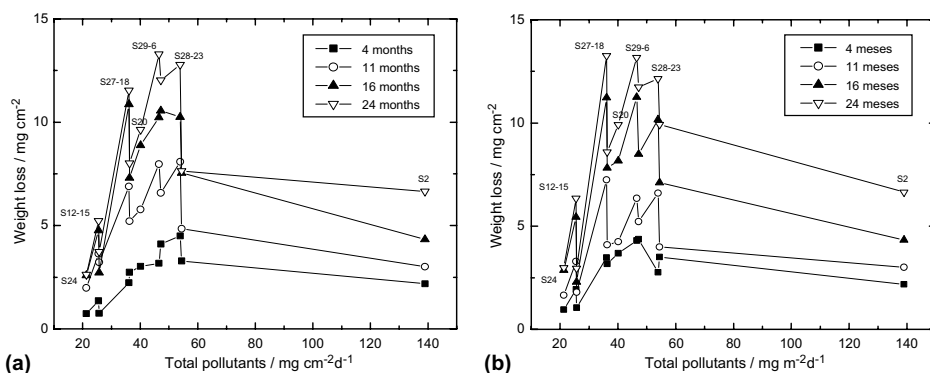


Fig. 12. Weight loss of aluminium and AA6201 alloy in the 11 marine stations as a function of the total pollutant content of the test sites, for the four distinct exposure times. (a) Aluminium. (b) AA6201 alloy.

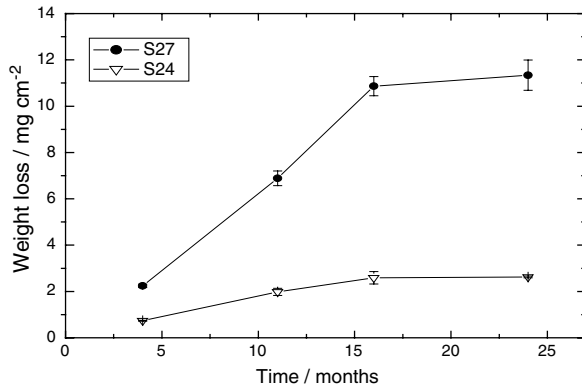


Fig. 13. Weight loss deviation of aluminium in marine stations 24 and 27.

When a similar analysis is performed on samples exposed in the marine-industrial test sites, however, as all sites are nearer the sea shore line and at more uniform heights over sea level, less evident TOW differences would be noticed amongst them. Also, the much higher  $\text{SO}_2$  as compared to the  $\text{Cl}^-$  contents with higher dew condensation relative to the various marine sites would not originate such aggressiveness scattering in the pollutants effect. For these 6 sites the TOWs on the metallic samples would probably dissolve more pollutants available, manifesting the aggressive  $\text{Cl}^-$  and greater  $\text{SO}_2$  effect more homogeneously in all these sites. Thus, higher maximum weight losses were determined in these 6 stations than at the 11 marine sites, evidencing a more effective corrosive effect by water dissolution of both pollutants added to higher  $\text{SO}_2$  levels in the atmosphere.

According to results summarised in Fig. 12 for all the marine atmospheres an additional weight loss would result as a function of the total pollutants, producing a rather cooperative, than competitive or synergic effect on both metals.

Rajagopalan et al. [31] found a non-direct correlation among the pollutant content in the atmosphere and in steel rusts formed there, being the washing-out effect of rains just before removal of each sample from outdoor exposure one of the reasons for such lack of correlation. This result was also previously found for these types of atmospheres [29]. The diverse effect of rains on the dissolution of the imbibed  $\text{Cl}^-$  and  $\text{SO}_4^{2-}$  produces uneven contents, according to local parameters of the test site. The most important among them are: soil pollution, wet-dry duration cycles, pollutants penetration in the inner phase of the rust, hydrolysis of the products formed, predominant winds modulating pollutants and wetting-drying duration cycles, etc.

The great amount of all possible combinations of these variables could give macroscopic results from synergistic to competitive interaction between  $\text{Cl}^-$  and  $\text{SO}_2$  when more than one pollutant is involved.

## 5. Conclusions

These results showed good correlation among corrosion rate, type and depth of attack and brittleness of the materials with respect to exposure time and content in both pollutants.

1. In both environments tensile strength to rupture showed an inverse relation with the weight loss for both metals.
2. Samples exposed at station 2, showed very low corrosion rate and high strength to rupture in spite of its highest chloride content.
3. Similar corrosion rate and mechanical resistance of both metals exposed to stations 2 and 12 were attributed to high adherence of the corrosion products formed at site 2.
4. Life expectancy is higher for alloy than for aluminium wires in all tested sites.
5. Corrosion products protectiveness increased with exposure time in marine atmospheres while it evidenced high adherence since the first exposure period in site 2, the marine atmosphere with highest  $\text{Cl}^-$  content.

## Acknowledgements

Chilquinta Energía and the Research Management of the Pontificia Universidad Católica de Valparaíso, Chile, financially supported this research project.

## References

- [1] F. Elshawesh, M. El Agaili, A. Elwaer, *Br. Corros. J.* 32 (1) (1997) 77–80.
- [2] A.S. Elola, T.F. Otero, A. Porro, *Corrosion* 48 (10) (1992) 854–863.
- [3] Aluminum with food and chemicals, *Compatibility Data on Aluminum in the Food and Chemical Process Industries*, third ed., The Aluminum Association, Inc., Washington, DC, 1975.
- [4] M. Morcillo, E.M. Almeida, B.M. Rosales, *ALUMINIUM* 76 (7–8) (2000) 610–615.
- [5] M. Morcillo, E.M. Almeida, B.M. Rosales, *ALUMINIUM* 76 (12) (2000) 1066–1070.
- [6] S. Feliu, M. Morcillo, B. Chico, *Br. Corros. J.* 36 (2) (2001) 157–160.
- [7] M. Stratmann, K. Bohnenkamp, W.J. Engel, *Corros. Sci.* 23 (1983) 969.
- [8] H.R. Copsin, *Proc. of the ASTM*, Philadelphia, 45 (1945) 2.
- [9] I. Suzuki, Y. Hisamatsu, N. Masuko, *J. Electrochem. Soc.* 127 (1980) 2211.
- [10] M. Poubaix, *Rapports Techniques CEBELCOR*, vol. 109, 1969, p. 1.
- [11] B.M. Rosales, E.S. Ayllón, in: W. Ailor (Ed.), *Atmospheric Corrosion*, John Wiley & Sons, Inc., 1982, p. 423 (Chapter 29).
- [12] B.M. Rosales, E.S. Ayllón, in: W. Ailor (Ed.), *Atmospheric Corrosion*, John Wiley & Sons, Inc., 1982, p. 501 (Chapter 35).
- [13] B.M. Rosales, E.S. Ayllón, in: W. Ailor (Ed.), *Atmospheric Corrosion*, John Wiley & Sons, Inc., 1982, p. 415 (Chapter 28).
- [14] ISO 9223, *Corrosion of metals and alloys, Classification of corrosivity of atmospheres*, ISO, Geneva, 1991.
- [15] ISO 9224, *Corrosion of metals and alloys, Guiding values for the corrosivity categories of atmospheres*, ISO, Geneva, 1991.
- [16] ISO 9225, *Corrosion of metals and alloys, Corrosivity of atmospheres—methods of measurement of pollution*, ISO, Geneva, 1991.
- [17] ISO 9226, *Corrosion of metals and alloys, Corrosivity of atmospheres—methods of determination of corrosion rate of standard specimens for the evaluation of corrosivity*, ISO, Geneva, 1991.
- [18] ISO 8407, *Metal and alloys—procedures for removal of corrosion products from corrosion test specimens*, ISO, Geneva, 1992.
- [19] W. Koppen, *Climatología con un Estudio de los Climas de la Tierra*, Spanish version Pedro Henrich Pérez, FCE, México, 1948.
- [20] J. Richter, H. Kaesche, *Werk. Korros.* 32 (1981) 174.
- [21] G.C. Wood, J.A. Richardson, M.F. Abd Rabbo, L.P. Mapa, W.H. Sutton, in: R.P. Frankental, J.P. Kruger (Eds.), *Passivity of Metals*, The Electrochemical Society, Princeton, 1978.
- [22] J. Hitzig, K. Jüttner, W.J. Lorenz, W. Paatsch, *Corros. Sci.* 24 (1984) 945.
- [23] F. Mansfeld, M.W. Kendig, *J. Electrochem. Soc.* 135 (1988) 828.
- [24] K. Jüttner, W.J. Lorenz, W. Paatsch, *Corros. Sci.* 29 (1989) 279.

- [25] T.E. Graedel, *J. Electrochem. Soc.* 136 (1989) 204.
- [26] M. Morcillo, E. Almeida, B. Rosales, J. Uruchurtuy, M. Marrocos, Corrosion and protection of metals in the atmospheres of Ibero-America, Pare 1, CYTED, Madrid, 1998, p. 595.
- [27] J.R. Vilche, F.E. Varela, G. Acuña, E. Codaro, B.M. Rosales, A. Fernández y, G. Moriena, *Corros. Sci.* 37 (6) (1995) 941–961.
- [28] J.R. Vilche, F.E. Varela, G. Acuña, E. Codaro, B.M. Rosales, A. Fernández y, G. Moriena, *Corros. Sci.* 39 (4) (1997) 655–679.
- [29] R. Vera, B.M. Rosales, C. Tapia, *Corros. Sci.* 45 (2003) 321–337.
- [30] B.M. Rosales, *Mapas de Corrosividad Atmosférica de la Argentina*, first ed., América Editora, Buenos Aires, 1997, pp. 189–192.
- [31] K.S. Rajagopalan, S. Chandrasekanran, M. Sundaram, P.S. Mohan, in: *Proc. 5th. Int. Symposium on Modelling on Environmental Effects on Electrical and General Engineering Equipment*, Liblice, 1978, pp. 183–193.